Ocean Modelling 183 (2023) 102196

Contents lists available at ScienceDirect

Ocean Modelling

journal homepage: www.elsevier.com/locate/ocemod

The effect of uncertain river forcing on the thermohaline properties of the North West European Shelf Seas

Sarah E. Zedler [a,*], Jeff A. Polton [a], Robert R. King [b], Sarah L. Wakelin [a]

[a] National Oceanography Centre, Liverpool, United Kingdom
[b] Met Office, Exeter, United Kingdom

ARTICLE INFO

Keywords:
Regional modeling
River forcing
Shelf seas
Operational forecast
NEMO
Northwest European Shelf Seas (20W to 20E 40N to 65N)
Temperature and salinity

ABSTRACT

Modeling studies and observations show that the thermohaline properties of the North West European Shelf Seas (NWESS) are sensitive to surface wind and heat flux forcing, as well as river outflows that transport fresh water from land to the ocean. In previous studies, it was assumed that the variability of the thermohaline properties in response to river outflow could be adequately sampled with a high-resolution, submesoscale permitting, long-term (i.e., 30-year) deterministic hindcast. In this study, we assume that the statistical distribution of the river forcing, rather than the time series of forcing itself, is adequately constrained by a 28-year history (1991 to 2018) of river forcing created specifically for our domain. In this way, we created an ensemble of 10 lower-resolution (≈7-km), short-term (i.e., 2.5 years) hindcast models that are forced with randomly perturbed river outflows and an ensemble of surface fluxes from the 10-member ECMWF ERA5 reanalysis (the 'Test' ensemble) as well with a companion ensemble that is forced with the ERA5 surface forcing fluxes but unperturbed river outflows (the 'Base' ensemble) for the June 2016 through December 2018 time period.

In both ensembles, the modeled evolution of 25-hour averaged (to partially filter out tides) temperature and salinity is realistic with peaks in summer for sea surface temperature and in winter for salinity, and annual amplitudes that are comparable to those found in other studies of the NWESS. The increased mean and standard deviation of the sea surface and bottom salinity in the Test ensemble are partly an artifact of the assumption that the errors in river forcing have a log-normal distribution that mimics the episodic nature of river outflow with a positive mean and an asymmetrical shape with a long tail toward large values. For surface density, the standard deviation in the Test ensemble was below 0.5 kg/m3, covering an areal extent larger than that for the Base ensemble throughout the year. The annual cycle of the areal extent of density in that range had a peak in summer and minima in winter, in phase with that of the river outflow forcing. Overall, the effect of uncertain river forcing on the thermohaline properties in this study is small. In order to understand the true impact of river forcings, better temporal and spatial observations of river outflow are needed.

1. Introduction

The world's shelf seas comprise a relatively small area of the earth's ocean yet support a disproportionately large fraction of carbon sequestration, primary production, and commercial fisheries (Orton and Jay, 2005; Ridenour et al., 2019; Wakelin et al., 2020; Wu et al., 2021; Marta-Almeida et al., 2021; Sun et al., 2021; Skákala et al., 2022). The North-West European Shelf Seas have been studied extensively and shown to be sensitive to horizontal resolution (O'Dea et al., 2012, 2017; Graham et al., 2018), vertical resolution (Wise et al., 2022), the parameterization of sub-gridscale vertical turbulent mixing (Luneva et al., 2019), feedbacks between biogeochemistry and light attenuation schemes (Skákala et al., 2022), and tidally pulsed river outflow forcing (O'Dea et al., 2017). More generally, models with very high resolution (10 s to 100 s of meters) and idealized bathymetry, show that plume dynamics can be significantly altered via interactions with surface waves (Rodriguez et al., 2018; Moghimi et al., 2019), coalescence with nearby plumes (Warrick and Farnsworth, 2017), and the presence of a pre-existing coastal current (Jamshidi and Johnson, 2019b,a). For a comprehensive review of the dynamics of shelf seas, see Huthnance et al. (2022) and references therein.

Regions of freshwater input (especially in near-shore regions, also called ROFI) are very important to the biota, especially where shelf sea water is oligotrophic, because rivers transport biologically important nutrients (including iron, phosphate, and nitrogen), along with land-borne contaminants and sediments. To date, observations of river

* Corresponding author.
E-mail address: sarah.zedler@gmail.com (S.E. Zedler).

https://doi.org/10.1016/j.ocemod.2023.102196
Received 12 January 2023; Received in revised form 15 March 2023; Accepted 28 March 2023
Available online 6 April 2023

inflow have been spatially and temporally sparse. At the same time, the ability of a single prognostic model to accurately forecast the shelf sea state is constrained by uncertainties in sub-surface parameterizations, boundary and surface forcing, the bottom drag coefficient, and by the sparseness of temperature and salinity observations, particularly below the surface. Most of the theoretical and laboratory experiments agree on the basic plume dynamics and structure (e.g., Horner-Devine et al., 2015) including the introduction of several nondimensional scales that help categorize individual river outflow types (e.g., Garvine, 1995; Horner-Devine et al., 2006; Poggioli and Horner-Devine, 2018; Jamshidi and Johnson, 2019a,b; Basdurak et al., 2020; Spicer et al., 2021). Our ≈7-km grid domain of the NWESS does not resolve all of the length scales that are present in a plume wake, nor the full set of small rivers (e.g., with outlets in UK) . Specifically there are no internal tides in our model such as found in mesoscale-permitting models of the NWESS (Guihou et al., 2017). However, there is considerable value in understanding the effect of uncertain river forcing in our AMM7 domain, as part of a broader effort considering those of other uncertain forcings (as mentioned above), especially as our model is an operational ocean forecasting model used at the UK Met Office. If river forcing is important, then we will need to increase the density of observations.

The purpose of this study is to understand the impact of variations in river flow pulses, as well as surface flux forcings, on the temperature and salinity in the North West European Shelf Seas (NWESS). The NWESS have been studied extensively (e.g., Huthnance et al., 2022), but the relationship between thermal and haline response to surface river fluxes needs to be better understood. Here, we investigate the ensemble statistics from a set of realistic prognostic models. We explore the effects of uncertain surface forcing fluxes and river forcing on the temperature and salinity. We use a 28-year history (1991 through 2018) of daily river inflow (from a total of 172 river inlets) to build an ensemble of river forcings with realistic statistics. These ensembles are used to force a 7-km configuration of the NWESS, using the Nucleus for European Modeling of the Ocean (NEMO) framework (Madec, 2008). We set up two 10-member ensembles which are forced by an ensemble of 10 realistic, prescribed surface flux forcing from the ERA5 ensemble of surface fluxes (Hersbach et al., 2020). In the 'Base' ensemble, each model was forced with unperturbed river forcing from a 28-year outflow history created specifically for our domain (referred to as NOWMAPS, for details see Section 3, the subsection entitled 'Observational River Database'). A companion ensemble (referred to as the 'Test' ensemble) was modified to include the addition of realistic flow pulses in river forcing with the same statistics (i.e., standard deviation and mean) as in the NOWMAPS river history.

The 'Base', ensemble members would only be expected to exhibit realistic spread in the evolution of the temperature and salinity fields, particularly below the mixed layer or for salinity at any depth. Work is ongoing at the Met Office to include additional perturbations to produce an ensemble with realistic spread (e.g., including stochastic model physics schemes and lateral boundary conditions from a global ensemble), as done int the Met Office global ensemble system. We prioritized an investigation of river forcings, because the effects of other uncertain forces were known to induce biases in the ocean state (e.g., Luneva et al., 2019). Our river ensemble is a preliminary framework being used here to perform sensitivity experiments, and has not been optimized for any specific variable.

2. Model details

The ensemble members employ version 3.6 of the NEMO (Madec, 2008) and are configured for the 7-km resolution, 51 (terrain following) depth layer, Atlantic Margin Model domain (AMM7, shown in Fig. 1; O'Dea et al., 2012, 2017) during the June 2016 through December 2018 time period. Note that in this paper, the analysis is based only on December 2017 through December 2018 to allow the regional model ocean physics to adjust to the surface forcing.

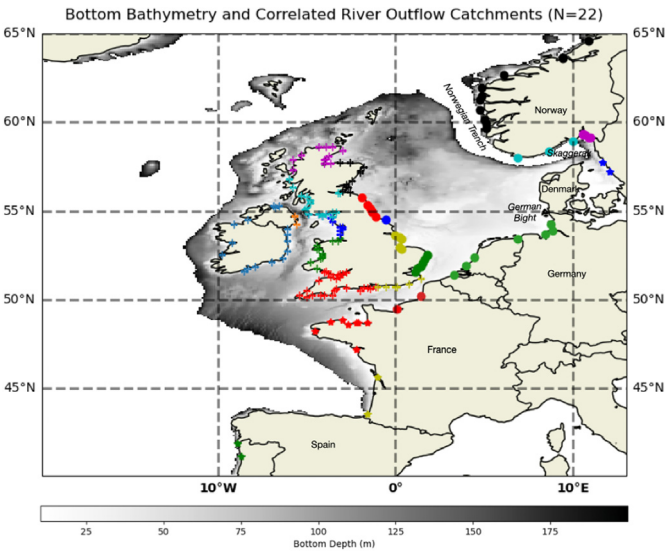

Fig. 1. The bottom bathymetry of the North West European shelf seas. Rivers are grouped into 22 separate catchments where each river in a catchment has a correlation coefficient larger than 0.3. The river catchments each have a unique marker and color. Depths below 200 m are masked out.

The bathymetry of our domain (shown Fig. 1) is spatially variable, supporting a wide range of hydrographic conditions from year-round tidally mixed vertical homogeneity to a seasonally stratified water column in spring and/or summer. The geographic positioning of the United Kingdom (also referred to as UK) allows the exchange of water between the shelf seas and the relatively warm, salty Atlantic water on the west, and the relatively cold, fresh water from the Skagerrak and German Bight to the east. This allows the opportunity for different types of instabilities to develop, including barotropic, baroclinic, symmetric, frontogenesis, and shear-driven mixing.

It is noteworthy that the spatial density difference (from east to west) would have been larger if not for compensating effects (for density) of temperature and salinity in both of these water masses. However, the full spatial and temporal range of dynamics is not resolved with our 7-km resolution, as the first baroclinic Rossby radius is about 6 km on the shelf (Chelton et al., 1998; Holt et al., 2017). Specifically, a field of energetic internal tides with peak temporal variability at quarter- and semi-diurnal as well as diurnal timescales as found in observations is absent in our model (Guihou et al., 2017).

Vertical turbulent mixing is parameterized using the generic length scale scheme (O'Dea et al., 2017; Luneva et al., 2019). The lateral and surface boundary conditions, tidal forcing, and harmonic/biharmonic viscosities and other model setup details are the same as in King et al. (2018).

3. Ensemble setup

Two 10-member ensembles are set up to investigate the effect of uncertain river forcing on the thermohaline properties of the NWESS. Both ensembles are forced with the prescribed, 3-hourly surface heat and wind fluxes, atmospheric pressure, and precipitation minus evaporation from the 10-member, ≈31-km resolution, ERA5 ensemble described in Hersbach et al. (2020), so that there is a one-to-one correspondence between the Base and Test ensemble members with identical forcing.

The first ('Base') ensemble is forced with unperturbed NOWMAPS river outflow history, whereas its' companion ('Test'), includes the addition of ensemble-member dependent random, daily, realistic perturbations to the river outflow time series, as described below. Both ensembles adopt the framework from an evolved prognostic (i.e. non-data assimilative), tidally-forced, physics-only version of the United Kingdom Meteorological Office FOAM-Shelf v9 ensemble (referred to as the UK Met Office ensemble O'Dea et al., 2017; King et al., 2018).

Observational river database. The NOWMAPS river discharge data (with 172 outlets) are produced from an updated version of the river dataset used in Lenhart et al. (2010) combined with the climatology of daily discharge data from the Global River Discharge Data Base (Vörösmarty et al., 2000) and from data prepared by the Centre for Ecology and Hydrology as used by Young and Holt (2007). In other observational data sets developed for higher resolution models, there were over 300 river outflow points and larger total discharge overall (O'Dea et al., 2017; Graham et al., 2018). The treatment of two or more closely spaced (i.e., subgridscale) small rivers as one outlet likely affects the physical evolution of the buoyant plume. The two hydrographic settings can have very different physics (Warrick and Fong, 2004; Warrick and Farnsworth, 2017). On days where observations were unavailable, the NOWMAPS river outflow defaults to the climatological annual cycle of the available data. It is worth noting that in 2018, when the NOWMAPS river history was compiled, the observational database was incomplete. Of particular note, there were no available data for rivers sourced in the United Kingdom after 2014. This is one reason why the spatially summed river records for 2017 and 2018 are, relative to other years, close to the climatological mean (Fig. 2). When this is the case, the variability in the NOWMAPS dataset is likely underestimated.

The 172 river outflow timeseries in the NOWMAPS reanalyses are not strictly statistically independent from one another. Each river belongs to one of 18 river districts (as shown in Fig. 1 of Lane et al., 2022), and can be grouped into 22 statistically independent catchments where the temporal cross-correlation coefficient between any two river outflow records within a catchment is ≥0.3. This suggests that the number of degrees of freedom in the NOWMAPS river database – about 20 – is much smaller than the number of rivers. The largest catchment includes the Cornwall peninsula (red crosses in Fig. 1), an area broadly covering the region from 6W to 1.1W and 50N to 51.6N with 26 rivers.

River perturbations. For the Base ensemble, each member is forced with river outflow from a new daily, 28-year observational reanalysis (1991–2018) created specifically for the AMM7 domain at the Plymouth Marine Laboratory as part of the NOWMAPS project. The Test ensemble is forced with realistically perturbed NOWMAPS rivers.

We assume that the daily river runoffs have a log-normal distribution (in time) as found previously (Bowers et al., 2012), with a very long positive tail toward large numbers to represent the episodic nature of storms (1–3 days) as well as a seasonally-varying nonzero mean. The perturbed river runoff r' is calculated in Eq. (1)

$$log(r') = log(r) + log(r''(\sigma, \mu)) \tag{1}$$

where r is the observed river runoff and r'' is a sample from a (reproducible) random variable with mean μ and standard deviation σ defined for each river and year day, as shown for the Rhine River in Fig. 3. The random seed is uniquely determined for each river, ensemble member, and year day. This allows us to assess the effect of uncertain river forcing on the hydrography by direct differencing of the Test and Base ensemble members. In each ensemble, the first member is forced with the unperturbed NOWMAPS river runoff reanalysis, which means that they are identical, and are therefore omitted from comparisons between the two ensembles. As a proxy for each individual river, we demonstrate that the total daily outflow (spatially summed at each timestep with N = 172) has a strong seasonal cycle with a maximum in the winter, a secondary (precipitation associated) peak in spring, and a minimum in summer as well as an approximate log-normal distribution (Fig. 2). Notably, the seasonal mean in the total daily river outflow is roughly six months out of phase with that of solar insolation. This implies that freshwater input and solar insolation have competing effects on the sea surface density in winter and summer, but complimentary effects during the transitional seasons.

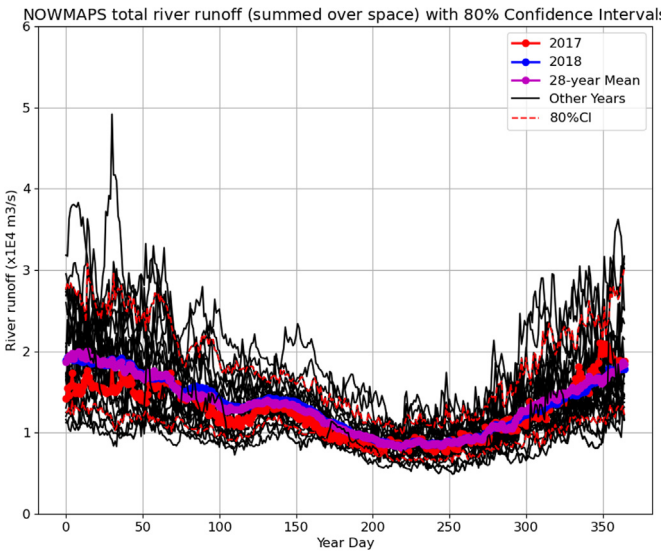

Fig. 2. The timeseries of the total (spatially-summed) river runoff as a function of year day for the 28 year period from 1993 to 2018 in black, as well as the 80% confidence intervals (N = 28) in dashed red lines, the climatological annual cycle (magenta circles), the 2017 record in red circles, and the 2018 record in blue circles.

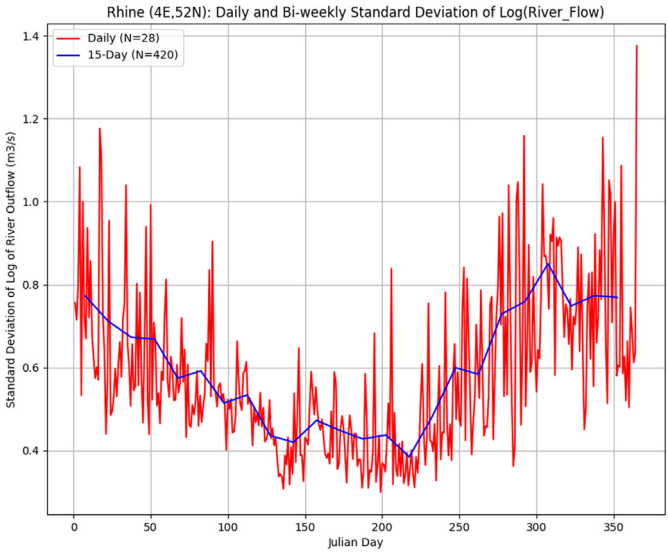

Fig. 3. Time series of actual standard deviation (N = 28 years) of runoff for the River Rhine along with the smoothed linear fit.

Justification for river perturbations. The arithmetic mean and standard deviation of the total outflow have strong seasonal cycles (Bowers et al., 2012). As is characteristic for log-normal distributions, that of the year-day mean of the total river runoff (relative to the daily mean) is uneven with a longer tail above the mean than below it. The mean auto-decorrelation time scale for the total river outflow is 2 days. However, the mean auto-decorrelation time scale for each river (with a 0.5 criterion) is 7 to 15 days. We subsample the total river outflow every 2 days after dividing the time series into 4 90-day periods. The distribution (i.e., frequency histogram) of the total river outflow is statistically indistinguishable to that of a companion sample (Nsamp = 10 000) with the same mean and standard deviation (with a Kolmogorov–Smirnov statistic of 0.03 and a p-value ≥ 0.05). The standard deviation of the river outflow (shown in Fig. 3 for the Rhine river) as a function of year-day (based on 28 samples per day) has a strong annual cycle, but is also very variable at daily timescales

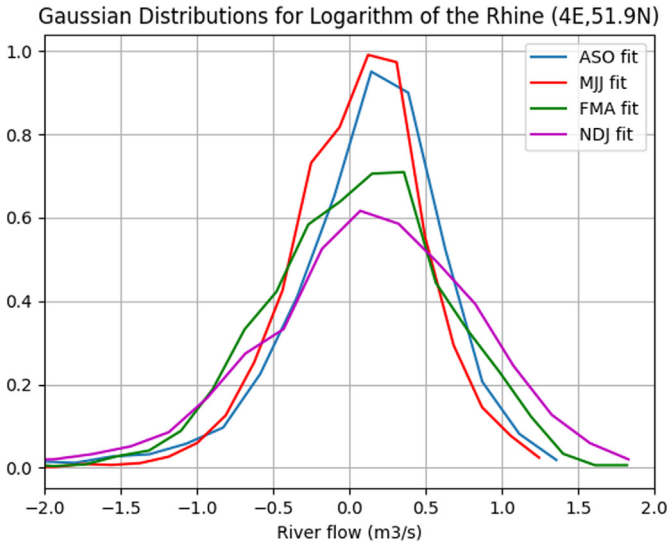

Fig. 4. Seasonal distributions of the logarithm of river flow to fit the observations.

(Fig. 3). This is what we would expect given our small sample size (Fig. 3). Given the 15-day decorrelation timescale, we take a straight 15-day average of the standard deviation timeseries (so that there are 420 15-day values with N = 28) to reduce and smooth the temporal variability in the river flow, while maintaining the annual cycle. We then fit a Gaussian distribution to the histograms of the logarithm of river outflow for 420 15-day records in each month, regardless of year.

As a demonstration of the annual variability of the statistics of the 15-day cycle, we show seasonal means (for the Rhine) of the distribution (Fig. 4) which have been subsampled on 30-day time scales, so that they are temporally statistically independent of one another. The distribution is widest in the winter, narrowest in the summer, and somewhere in-between during the transitional fall and spring season. The rivers are not perfectly log-normally distributed (see Fig. 3), and might be equally modeled as a power distribution (Bowers et al., 2012).

4. Characterization of on-shelf seasonal cycle in base ensemble

First we present output from the Base ensemble. We begin by considering the on-shelf (where bottom depth is ≤200-m) seasonal mean of a monthly subset of partially tidally-filtered 25-h records from the Base ensemble (Figs. 5 and 6). The thermohaline properties of the NWESS have realistic pronounced seasonal cycles in all of the ensemble members.

Density calculation. Density was calculated offline from 25-h averaged temperature and salinity using the Lindström et al. (2010) UNESCO equation of state, before calculation of the standard deviation in the ensemble dimension.

Temperature. In winter, the water is vertically homogeneous for salinity and temperature. In spring, there is an increase in SST (of about 2 °C) in keeping with increased day length. In summer, the surface temperatures range from around 12 °C to 19 °C, with the shallow waters of the NWESS remaining vertically homogeneous. The deeper waters exhibit a layer of warm surface water overlying the tidally-mixed interior. As fall approaches, the surface mixed layer is then eroded as day length decreases and storms increase in frequency and intensity. Spring and fall are transitional periods with warm water (south of 55°N) along the southwest shelf break.

Salinity. In all seasons, there is salty water on the west side of the UK (Atlantic shelf) and in the Irish Sea, and relatively fresh water fed by rivers. Other sources of fresh water include (local) precipitation and transport through the Baltic Boundary. In general agreement with observations and models, variability in SSS that is attributed to wind forcing uncertainty is large on the break between the NWESS and the Norwegian Trench (Davies and Heaps, 1980; Pingree and Griffiths, 1980; Ikeda et al., 1989). The annual cycle of SSS in the Base ensemble is relatively small or unremarkable (Fig. 6). The shallow, year-round vertically-homogeneous English Channel that connects the east and west water masses in the south of the domain has intermediate salinity with an east west salinity difference of about 7 ppt. Around the UK, a swath of shallow fresh water from river inflows increases in spring and summer. This probably relates to the formation of a barrier layer with stratification – specifically, there is westward movement of the 34.6-ppt halocline.

Density of sea water. At different times of year, the temperature and salinity have additive or compensating effects on the density. This is because the annual cycle for temperature is highly variable relative to that for salinity. In winter, cold salty waters have additive effects on the density in the western part of the domain but competing effects in the east, whereas the opposite is true in summer. During the transitional seasons, the effects of salt and temperature are compensatory. Nevertheless, when expressed in density equivalent units (i.e., normalized by the temperature expansion or haline contraction coefficient), the differences in the two ensembles are almost entirely attributable to salinity. This is not surprising, considering that any temperature difference between the two ensembles would likely be a secondary effect (from, e.g., the combination of a too shallow barrier layer and subsequent insufficient vertical mixing), whereas the salinity is perturbed directly.

The seasonal cycle of sea surface and bottom salinity serves as a proxy for the degree of mixing (not shown). In winter and spring the water column is vertically homogeneous due to tidal mixing. In summer and fall the north part of the North Sea (as far south as 55°N) is weakly stratified with a fresh, warm (i.e., barrier) layer on top.

5. Characterization of on-shelf differences between ensemble means

The difference in the ensemble means for SSS and SST in January 2018 and July 2018 show that, as expected, perturbed river outflows predominantly affect the salinity, without changing the temperature by much (Fig. 7). The amplitude of this anomaly is on the order of 0.1–0.2 ppt. Interestingly, the anomaly in the ensemble mean of SST has a patchy spatial pattern across the domain, whereas the SSS anomaly is tightly confined near the coast.

6. Characterization of on-shelf variability to pulsed river forcing

Next, we present the results of perturbing the river inflows. We focus our discussion on the variability of temperature and salinity in January, and July, of 2018, as representative as the extrema (or amplitude) of the annual cycle. Because we started the model in June, 2016, some of the summertime surface effects from the previous year (i.e., 2017) will have had the opportunity to be mixed to depth by July 2018. We consider the standard deviation for each of these variables at the sea surface and bottom (Figs. 8 and 9 for temperature, and Figs. 10 and 11 for salinity).

Overall, the magnitude of the standard deviation fields for temperature and salinity are of the same order in the Base and Test ensembles (comparing the left and right columns of each of Figs. 8 through 11). In winter, the surface and bottom statistics are very similar (compare top and bottom panels in Fig. 8 and in Fig. 10), whereas they have more pronounced differences in July (compare top and bottom panels in Fig. 9 and in Fig. 11). By consideration of the direct differences of the standard deviation between the Test and Base ensembles, we can gauge the impact of perturbing rivers on the statistics of the thermohaline properties of the NWESS.

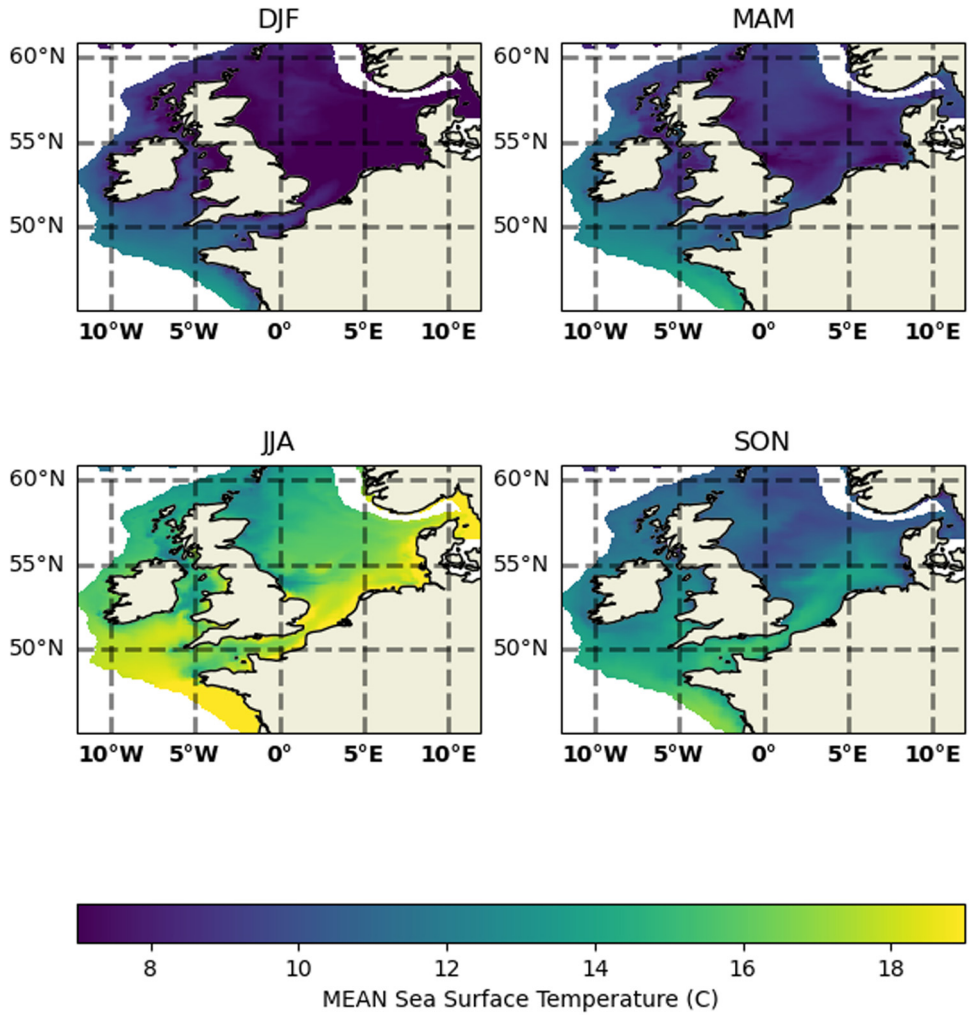

Fig. 5. Seasonally and temporally averaged 25-h ensemble mean of sea surface temperature (SST) for Base ensemble. Upper left: for winter (DJF). Upper right: for spring (MAM). Lower left: for summer (JJA). Lower right: for fall (SON).

Temperature. In winter, the effect of perturbing river inflow on the variability of the temperature field is on the order of 0.15 °C at both the surface and the bottom, as one would expect for a vertically homogeneous, tidally mixed basin (see colorbars for left panels in Fig. 8). The effect of additionally perturbing rivers results in increased variability in some areas along the west coast of Scotland and the west coast of western Europe (right columns of Fig. 8). Variability of sea surface temperature in the vicinity of the Norwegian trench shelf can be either larger or smaller in the two ensembles. The following summer, the standard deviations for temperature in the Test and Base ensembles are enhanced, particularly in the southern North Sea in the region of the west coast of Germany.

Salinity. Year round there is a freshwater anomaly between 0 and 0.2 ppt in the ensemble mean SSS for the Test ensemble relative to that in the Base ensemble (Fig. 7), accompanied by seasonal variability of comparable magnitudes but different spatial patterns (see left panels of Fig. 10).

Of possible evidence of summertime stratification, the region of the shelf seas with the largest standard deviation for salinity is at the surface, along the slope shelf of the Norwegian trench (Fig. 11). This surface peak is not present at the shelf sea floor. In general, the spatial patterns of the freshwater anomalies in the mean have maxima near coastlines of the UK, Ireland, or western Europe (starting northward of 45°N) just to the north of the border between Spain and France, decaying in the offshore direction. These characteristics likely reflect the fact that the river inflow perturbations are drawn from a log-normal distribution. The assumption that the river inflows have a log-normal distribution conserves natural variability but not volume of seawater. The patterns in both the surface and bottom anomalies are tightly constrained to the coast of the UK and the European shelf seas. This is likely, in part, an artifact of the combination of low horizontal resolution that inadequately resolves the dynamics of the river plumes, forcing them to be surface advected (Horner-Devine et al., 2015; Yankovsky and Chapman, 1997) and to contribute to a (horizontally) thin geostrophic coastal current, as suggested in Graham et al. (2018), and in part due to the fact that standard deviation of freshwater input of rivers is largest at the coastal river outlets (shown in Fig. 1). The percentage of variability in the anomaly between the Test and Base ensembles relative to the Base ensemble ranges from zero to 20%. In winter there is virtually no difference in the hydrography because the water column is vertically homogeneous. The largest values of the fractional variability are in spring and summer when there is appreciable near-surface vertical stratification.

Density. Over much of the domain, the standard deviation in surface and bottom density is below 0.05 kg/m^3 (surface map shown in Fig. 12). However, there are regions where the standard deviation in density is as high as 0.5 kg/m^3, especially in July when stratification is at a maximum for both salinity and temperature. The annual cycle of the total (spatially-summed) area where standard deviation in density is in the range 0.05 to 0.5 kg/m^3 is shown in Fig. 13. This measure

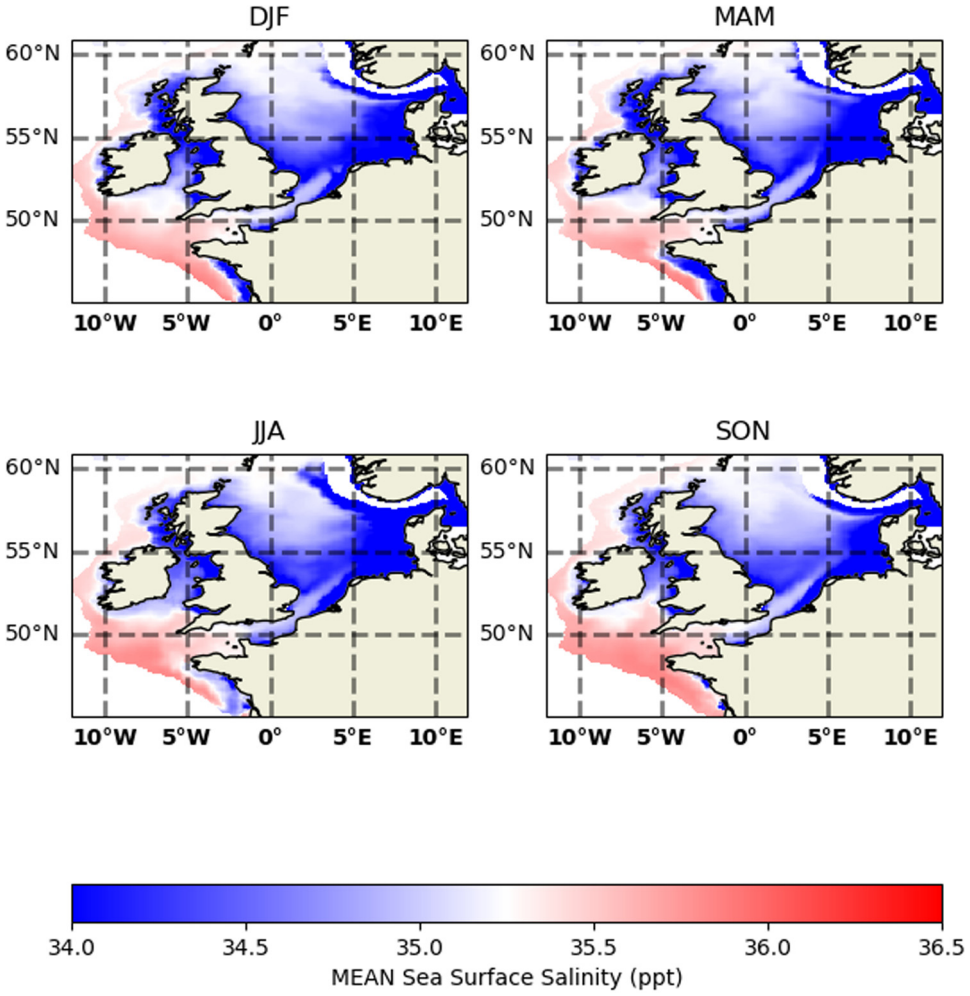

Fig. 6. Seasonally and temporally averaged 25-h ensemble mean of sea surface salinity (SSS) for Base ensemble. Upper left: for winter (DJF). Upper right: for spring (MAM). Lower left: for summer (JJA). Lower right: for fall (SON).

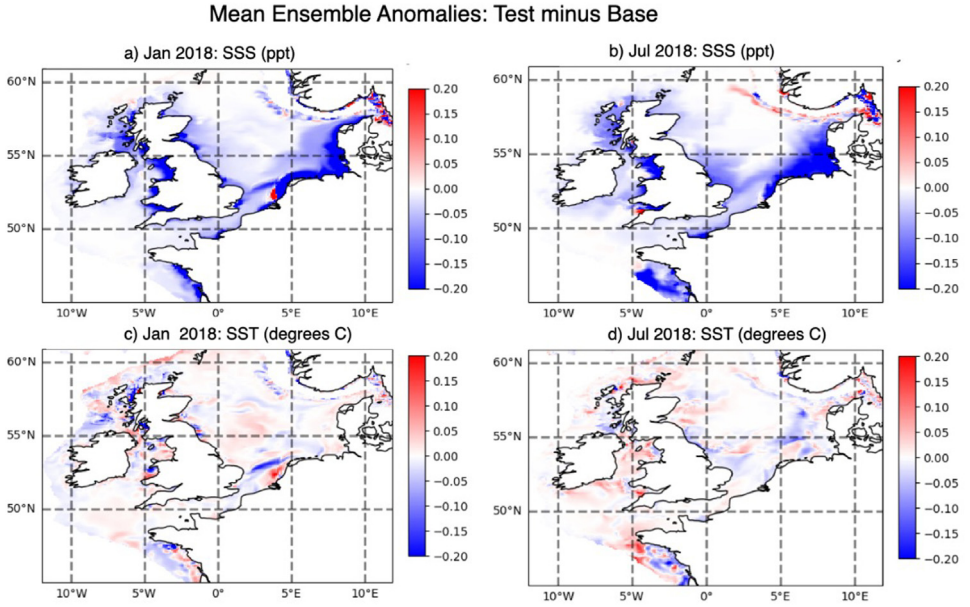

Fig. 7. Anomaly of 25-hour-averaged ensemble mean of sea surface salinity (SSS with units ppt) and sea surface temperature (SST with units C) between the Test and Base ensembles: Test minus Base. (a) SSS for January (b) SSS for July (c) SST for January (d) SST for July.

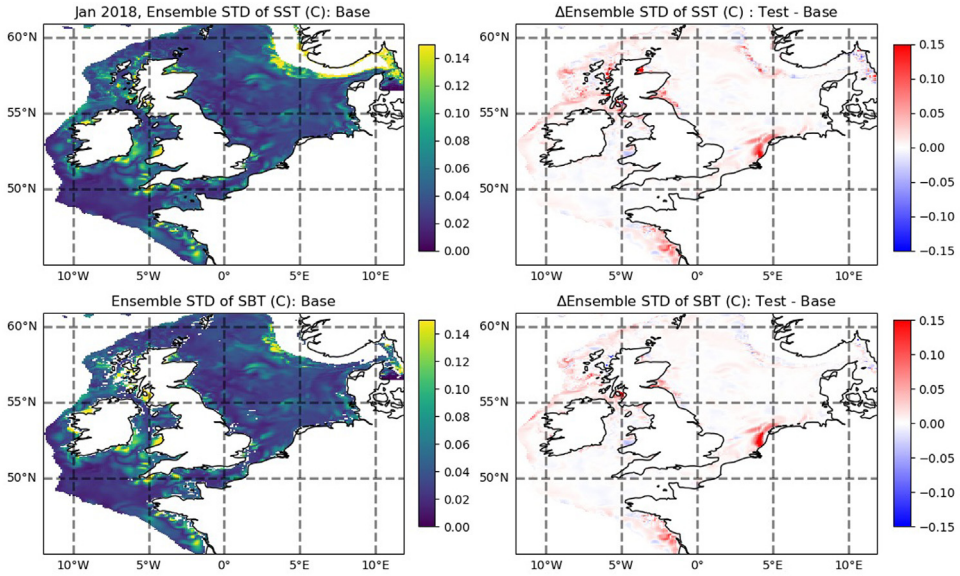

Fig. 8. January 2018 standard deviation of 25-hour-averaged sea surface (top row) and bottom (bottom row) temperature for Base ensemble (left column) and the difference between the Test and base ensembles (right column).

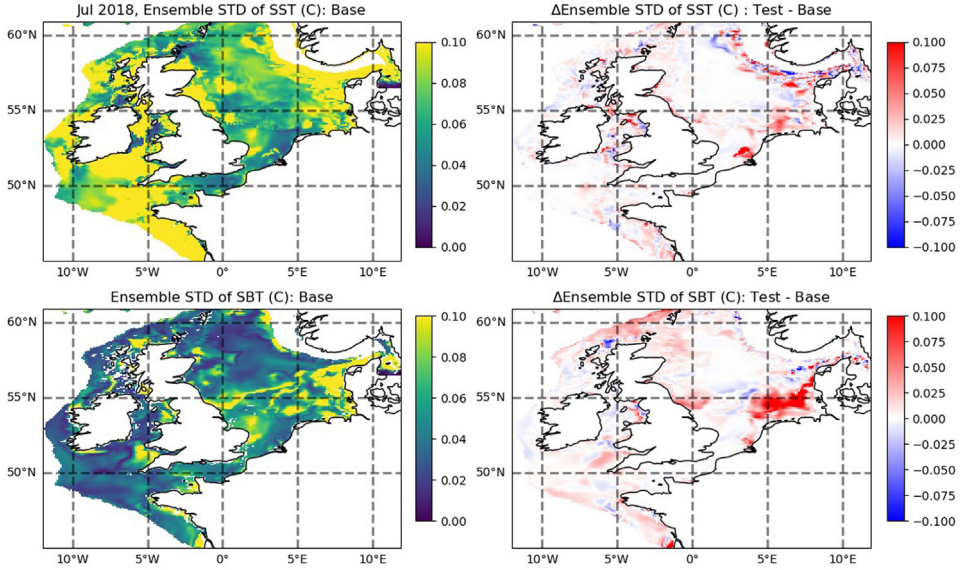

Fig. 9. July 2018 standard deviation of 25-hour-averaged sea surface (top row) and bottom (bottom row) temperature for Base ensemble (left column) and the difference between the Test and Base ensembles (right column).

shows that there is a larger area of sea surface variability in density in the Test, than in the Base, ensemble. Notably we consider it a metric that indicates the differing spatial extents of density variability for each ensemble. In both ensembles, the time series of the surface areal density variability index has maxima in June or July and minima in winter, with amplitudes (maximum minus minimum) of 0.19% and 0.28% in the Base and Test ensembles (Fig. 13).

7. Discussion

To put our work in context with other studies, in the following, we will compare our ensemble statistics for SSS and SST with those from 30-year non-data assimilating deterministic models on the AMM7 grid and also the mesoscale-resolving AMM15 grid. From the first comparison, we will show that there is a need for higher temporal and spatial density of river outflow observations. From the second comparison, we will conclude that the resolution of internal tides in the AMM15 domain does not dramatically reduce the bias in the temporal mean for SSS and SST. The lack of a significant decrease in biases in SSS and SST on the 1.5-km grid will suggest that resolution of the field of internal tides – which represent episodic short length- and time-scales – does not affect the associated biases by much. This could indicate that most of the mixing in the AMM15 model is in the vertical, rather than the horizontal, dimension.

Comparisons with other modeling studies using AMM7 grid. As part of a progression of studies, O'Dea et al. (2017) showed that the long-term temporal average of thermohaline properties in a ≈ 12-km deterministic model of the NWESS had larger biases than those in a companion model on the AMM7 grid, and Graham et al. (2018) demonstrated that the biases in that same AMM7 model were of larger magnitude than those of a mesoscale-permitting model with ≈1.5-km resolution. Here we assume that the salinity biases have minimal (temporal) cumulative trend (or drift?) in O'Dea et al. (2017) and Graham et al. (2018),

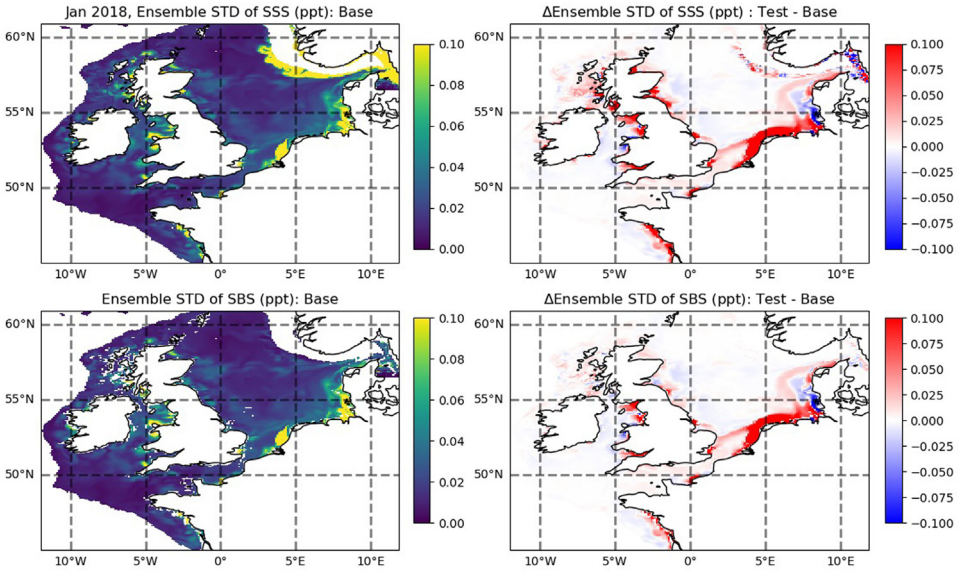

Fig. 10. January 2018 standard deviation of 25-hour-averaged surface and bottom SSS for Base ensemble.

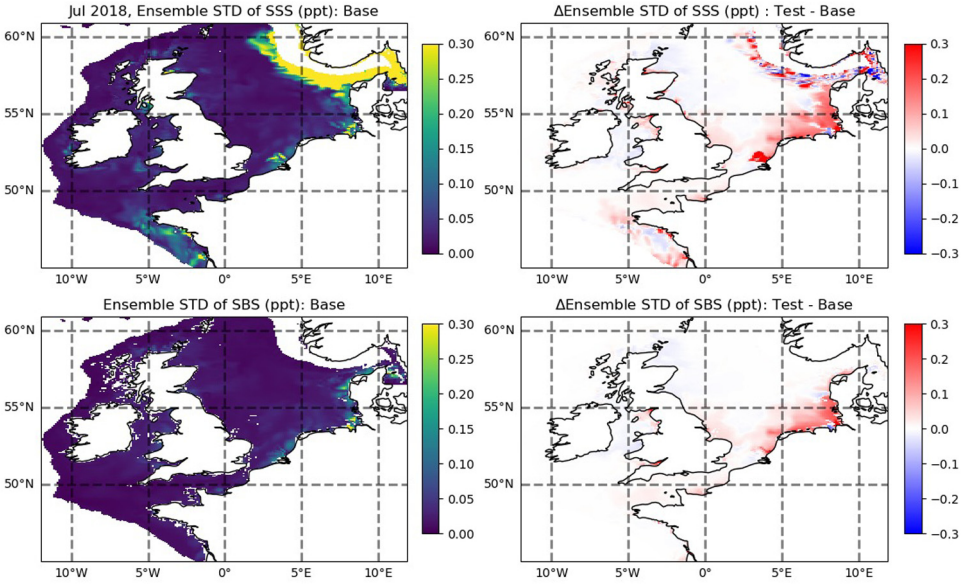

Fig. 11. Jul 2018 of 25-hour-averaged surface (top panels) and bottom (bottom panels) salinity for Base ensemble (left panels) and the anomaly in STD between the Test and Base ensembles (right panels).

Nonlinear feedbacks could occur via formation of a barrier layer in summer with too-large freshwater anomaly at the surface coupled with too little (parameterized sub-gridscale) vertical turbulent mixing. To the extent that anomalies in our ensemble means for SSS (Fig. 7a and b) and SST (Fig. 7c and d) essentially isolate the effect of river outflow forcing, we can compare them to the biases in O'Dea et al. (2017) and Graham et al. (2018) and ask whether they have the appropriate size and amplitude to reduce or increase the bias. The answer is that the range in the magnitude of the anomaly in SSS is about 10% of that in the seasonal bias shown in Fig. 7 of O'Dea et al. (2017) and that of the interannual mean of Fig. 4 of Graham et al. (2018), while that of the SST is negligible (ranging between −0.05 and 0.05 °C). Whether or not the bias in the means of our anomaly in SSS is of the appropriate sign to reduce biases is a function of location. Around the United Kingdom, the anomaly of the (ensemble) mean SSS is of the correct sign to reduce the biases (Fig. 7a and b). However, on the west coast of Europe and along the Norwegian trench, the anomaly in our ensemble mean is of the same sign of the biases found in Graham et al. (2018) and O'Dea et al. (2017), which, taken together, would act to increase the bias even further.

Note that these anomalies in the ensemble mean of SSS are likely due to differences in the river forcing employed in O'Dea et al. (2017) (see their Fig. 3) and the river outflow records for June 2016 through December, 2018 used in our study. For instance, in O'Dea et al. (2017), the spatially summed E-HYPE rivers used to force their AMM7 model were overall 18% larger than in the CO4 climatology described in O'Dea et al. (2012). Additionally, there was considerable variability in the spatial pattern of E-HYPE river outflows relative to the climatology. Particularly there were very large discharges on the west coast of Europe, but smaller variability around the east part of the UK (see their Fig. 4), whereas in 2017 and 2018 our river history is similar to the CO4 climatology (compare our Fig. 2 to Fig. 3 in O'Dea et al., 2017). The range of the total freshwater outflow for E-HYPE is between 1.2 and 3.8 m^3/s, whereas that for the CO4 climatological forcing between 0.8 and 2.2 m^3/s (see Fig. 3 from O'Dea et al., 2017). For comparison, the range of river outflows in our database are somewhere in-between

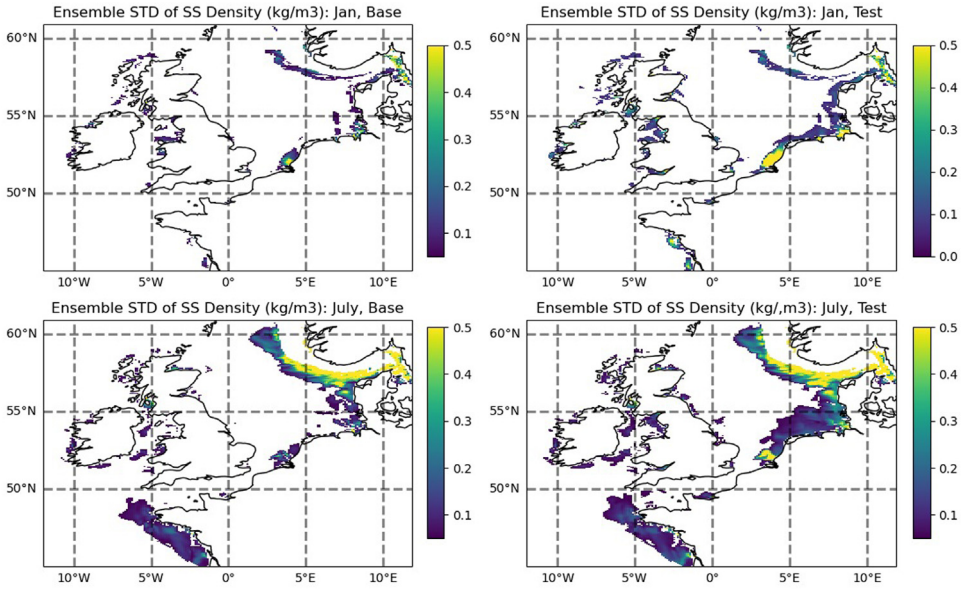

Fig. 12. Standard deviation of 25-hour-averaged surface density for Jan 2018 (top row) Jul 2018 (bottom row) standard deviation in the Base (left column) and Test (right column) ensembles. Regions with a standard deviation below 0.05 kg/m^3 are masked out.

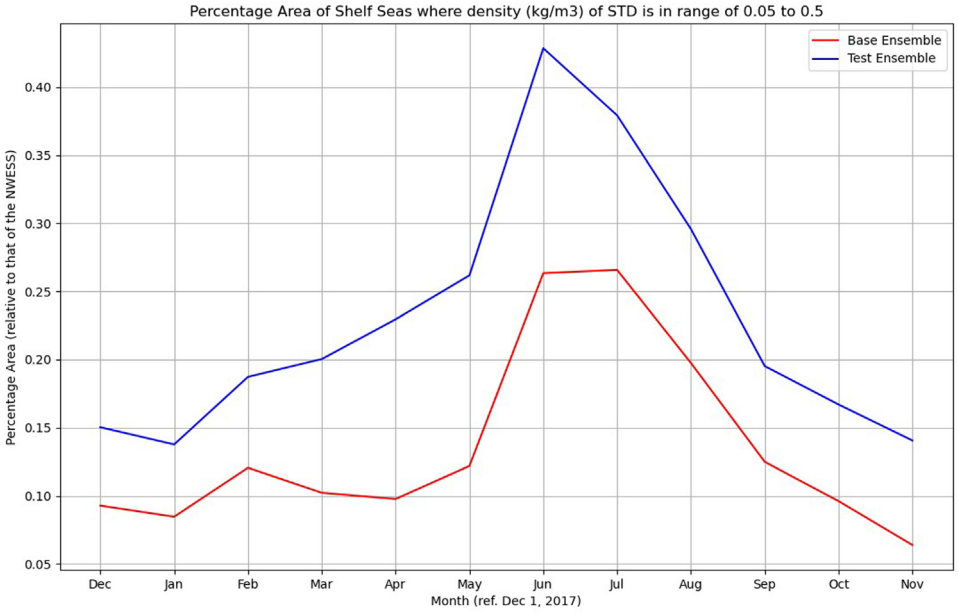

Fig. 13. Annual cycle of percentage total area where the standard deviation of density is larger than 0.05 kg/m^3.

the EHYPE database and CO4 climatology (to which it defaults when there is no available data), with outflows between 0.8 and 5 m^3/s, Fig. 2). Thus, we showed that relative to what was found in O'Dea et al. (2017), smaller, random, perturbations in river outflow result in relatively smaller differences in SSS of around 0.2ppt.

In summary, Graham et al. (2018) and O'Dea et al. (2017) found that river forcing can significantly impact the salinity properties of the ocean over a long time (i.e., 30-year) period, with SSS differences in the 30-year mean on the order of 1ppt (see Fig. 13c of O'Dea et al., 2017), between models forced with the E-HYPE river outflows, and those forced with the CO4 river outflow climatology with otherwise identical setup. This was larger than the effect of changing the Baltic Boundary condition (see Fig. 13d of O'Dea et al., 2017). The importance of rivers for modifying SSS then depends in large part on the accuracy of the river outflow history used to force them; clearly, river outflow histories are currently only poorly constrained by data. Our study, in agreement with others, collectively suggest that we need to increase the temporal and spatial sampling of rivers in the NWESS. In addition to river outflow, there are many other forcings that affect the thermohaline properties, that should also be considered in tandem. Accordingly, this work is part of a larger effort to characterize the effect of other uncertain forcings, such as the bottom boundary layer drag coefficient or the lateral boundary conditions for temperature and salinity. The effects of many of these forcings have been studied separately from one another (e.g., Skákala et al., 2022; Luneva et al., 2019). More could be learned from studying their complementary cumulative effects in an ensemble framework. They are likely responsible for non-linear feedbacks in the thermohaline properties of the NWESS.

Comments on the choice of horizontal resolution: AMM7 vs. AMM15 grid. We can also compare our anomalies in SSS to those in the AMM15 run as shown in Figs. 3 and 4 of Graham et al. (2018). Broadly

speaking, the anomalies in the ensemble mean SSS are weaker than the temporal mean in AMM15. The AMM15 ≈1.5-km mesoscale-resolving grid allows the resolution of a field of vigorous internal tides not present in AMM7. The advantage of AMM15 is that it resolves a wider range of dynamics, and presumably also has a better representation of the transfer of kinetic energy across length scales that can occur via nonlinear interactions. Indeed, in a comparison of observation-based power spectra of thermohaline variability for timeseries from a group of moorings on the shelf break in the Celtic Sea, with those from a ≈1.8-km degree regional model of the NWESS (Guihou et al., 2017), it was found that the energy peaks ranging between quarter–diurnal and diurnal periods were only well resolved in AMM15 (see their Fig. 7). The advantage of our approach is that the ensemble mean and standard deviation in our SSS and SST fields acknowledges the uncertainty in the forcings themselves; by comparing our results to AMM15, we can get a sense for the relative importance of accurate river forcing to increased horizontal resolution. In this study, the shorter time period of our model runs reduces any amount of cumulative drift in the model, which if large, could partially explain why our anomalies are so much smaller than found previously. In the AMM15 hindcast, the challenges posed for comparisons with observational data are different from those in our short-term model. One key issue is that the smaller scales resolved tend to be highly energetic and episodic in nature, which means that if the data and model share a feature (such as vertical undulations of the thermocline) that are spatially or temporally out of phase with one another, the difference between them can be very large. This is a huge problem for ocean data-assimilative forecasts as they move toward higher resolution.

8. Conclusions and future work

Using a new 28-year (i.e., 1993 through 2018) long daily river runoff history designed for forcing an ≈7-km model of the North West European shelf seas (for the AMM7 or Atlantic Margin Model Domain) in conjunction with the hindcast version of the UK Met Office operational shelf-seas forecasting system, we quantified the effect of uncertain river forcing on the thermohaline properties in an ensemble of non-assimilative hindcast ocean models for the December 2017 through December 2018 time period.

Comparing a 10-member (Base) ensemble with historical river forcing, to a companion (Test) ensemble that was forced with perturbed river outflows (drawn from a random distribution with standard deviation and mean equal to that of the 28-year history) we found only a small effect of uncertain river forcing on the ensemble mean and standard deviation of SSS of the NWESS by considering the direct differences between them for each ensemble member. The ensemble mean and standard deviation for SSS both had ranges of ≈0.2ppt, or about 10% that of the 30-year mean from a non-data assimilative deterministic hindcast model on the same grid. The effect on SST was negligible. The area where sea surface density was in the range between 0.05 and 0.5$\mathrm{kg/m^3}$, was larger in the perturbed ensemble than in the default. We explained these patterns by large differences in river forcing.

The ensemble framework can be used to calculate sample covariance matrices for implementation in data assimilation. This work is a step toward a more useful ensemble with realistic spread across different variables which has uses in both quantifying forecast errors, and in improving the data assimilation in operational forecasting systems. Further developments planned to the Met Office shelf-seas ensemble forecasting systems include introducing stochastic model physics perturbations, using lateral boundaries from the global ocean ensemble system, and updating the surface fluxes to use the Met Office atmosphere ensemble.

Work is also planned at the Met Office to use an improved shelf-seas ensemble within a hybrid ensemble/variational data assimilation scheme which combines climatological background errors with errors-of-the-day derived from the ensemble. This framework has been demonstrated in the Met Office global ocean forecasting systems and shown to have positive impacts (Lea et al., 2022).

Further modifications to the data assimilation method currently employed in both the regional and global ocean models (also known as 3D-var FGAT Waters et al., 2015), could include explicit estimation of model biases (calculated by an ensemble of models) which are later removed. Complementary efforts to improve assimilation methods in coupled physics – with atmospheric forcing (King et al., 2019), biology (Skákala et al., 2022), and atmosphere-land-ocean should continue. Recognizing that the open ocean and shelf seas have different dynamical regimes, further work is needed in the data assimilation method application in shallow waters.

CRediT authorship contribution statement

Sarah E. Zedler: Conceptualization, Methodology, Formal analysis, Investigation, Visualization, Writing – original draft, Writing – review & editing. **Jeff A. Polton:** Conceptualization, Methodology, Resources, Visualization, Writing – review & editing. **Robert R. King:** Conceptualization, Methodology, Formal analysis, Investigation, Writing – review & editing. **Sarah L. Wakelin:** Conceptualization, Methodology, Investigation, Writing – review & editing.

Declaration of competing interest

The authors declare that they have no known competing financial interests or personal relationships that could have appeared to influence the work reported in this paper.

Data availability

Data will be made available on request.

Acknowledgments

We thank Dr Sonja van Leeuwen (NIOZ Royal Netherlands Institute for Sea Research) for providing river discharge observations and Drs Yuri Artioli and Helen Powley (Plymouth Marine Laboratory) for preparing the NOWMAPS river data set. This work was supported by the CAMPUS project (Number NE/R006822/1).

References

Orton, P., Jay, D., 2005. Observations at the tidal plume front of a high-volume river outflow. Geophys. Res. Lett. 32, http://dx.doi.org/10.1029/2005GL022372.

Ridenour, N., Hu, X., Jafarikhasragh, S., Landy, J., Lukovich, J., Stadnyk, T., Sydor, K., Myers, P., Barber, D., 2019. Sensitivity of freshwater dynamics to ocean model resolution and river discharge forcing in the Hudson Bay Complex. J. Mar. Syst. 196, 48–64.

Wakelin, S., Artioli, Y., Holt, J., Butenschön, M., Blackford, J., 2020. Controls on near-bed oxygen concentration on the Northwest European Continental Shelf under a potential future climate scenario. Prog. Oceanogr. 187, 102400.

Wu, R., Wu, H., Wang, Y., 2021. Modulation of shelf circulations under multiple river discharges in the East China Sea. J. Geophys. Res. - Oceans 126, http://dx.doi.org/10.1029/2020JC016990.

Marta-Almeida, M., Dalbosco, A., Franco, D., Ruiz-Villarreal, M., 2021. Dynamics of river plumes in the South Brazilian Bight and South Brazil. Ocean Dyn. 71, 59–80.

Sun, D., Bracco, A., Liu, G., 2021. The role of freshwater forcing on surface predictability in the Gulf of Mexico. J. Geophys. Res. - Oceans 127, http://dx.doi.org/10.1029/2021JC018098.

Skákala, J., Bruggeman, J., Ford, D., Wakelin, S., Akpinar, A., Hull, T., Kaiser, J., Loveday, B., O'Dea, E., Williams, C., Ciavatta, S., 2022. The impact of ocean biogeochemstry on physics and its consequences for modelling shelf seas. Ocean Model. 172, 101976.

O'Dea, E., Arnold, A., Edwards, K., Furner, R., Hyder, P., Martin, M., Siddorn, J., Storkey, D., While, J., Holt, J., Liu, H., 2012. An operational ocean forecast system incorporating NEMO and SST data assimilation for the tidally driven European North-West Shelf. J. Oper. Oceanogr. 5, 3–17.

O'Dea, E., Furner, R., Wakelin, S., Siddorn, J., While, J., Sykes, P., King, R., Holt, J., Hewitt, H., 2017. The CO5 configuration of the 7km Atlantic Margin Model: large scale biases and sensitivity to forcing, physics options and vertical resolution. Geosci. Model Dev. 10, 2947–2969.

Graham, J., O'Dea, E., Holt, J., Polton, J., Hewitt, H., Furner, R., Guihou, K., Brereton, A., Arnold, A., Wakelin, S., Castillo-Sanchez, J., Mayorga-Adame, C., 2018. AMM15: a new high-resolution NEMO configuration for operational simulation of the European north-west shelf. Geosci. Model Dev. 11, 681–696.

Wise, A., Harle, J., Bruciaferri, D., O'Dea, E., Polton, J., 2022. The effect of vertical coordinates on the accuracy of a shelf sea model. Ocean Model. 170 (101935), 21.

Luneva, M., Wakelin, S., Holt, J., Inall, M., Kozlov, I., Palmer, M., Toberman, M., Zubkova, E., Polton, J., 2019. Challenging vertical turbulence mixing schemes in a tidally energetic environment: 1. 3-D shelf-sea model assessment. J. Geophys. Res. http://dx.doi.org/10.1029/2018JC014307.

Rodriguez, A., Giddings, S., Kumar, N., 2018. Impacts of nearshore wave-current interaction on transport and mixing of small-scale buoyant plumes. Geophys. Res. Lett. 45, 8379–8389.

Moghimi, S., Özkan Haller, H., Akan, C., Jurisa, J.T., 2019. Mechanistic analysis of the wave-current interaction in the plume region of a partially mixed tidal inlet. Ocean Model. 134, 110–126.

Warrick, J., Farnsworth, K., 2017. Coastal river plumes: Collisions and coalescence. Prog. Oceanogr. 151, 245–260.

Jamshidi, S., Johnson, E., 2019b. Vortex competition in coastal outflows. J. Mar. Res. 77, 325–349.

Jamshidi, S., Johnson, E., 2019a. Coastal outflow currents into a buoyant layer of arbitrary depth. J. Fluid Mech. 858, 656–688.

Huthnance, J., Hopkins, J., Berx, B., Dale, A., Holt, J., Hosegood, P., Inall, M., Jones, S., Loveday, B., Miller, P., Polton, J., Porter, M., Spingys, C., 2022. Ocean shelf exchange, NW European shelf seas: Measurements, estimates and comparisons. Prog. Oceanogr. 202, 102760.

Horner-Devine, A., Hetland, R., MacDonald, D., 2015. Mixing and transport in coastal river plumes. Annu. Rev. Fluid Mech. 47, 569–594.

Garvine, R., 1995. A dynamical system for classifying buoyant coastal discharges. Cont. Shelf Res. 15, 1585–1596.

Horner-Devine, A., Fong, D., Monosmith, S., Maxworthy, T., 2006. Laboratory experiments simulating a coastal river inflow. J. Fluid Mech. 555, 203–232.

Poggioli, A., Horner-Devine, A., 2018. Two-layer hydraulics at the river-ocean interface. J. Fluid Mech. 856, 633–672.

Basdurak, N., Largier, J., Nidzieko, N., 2020. Modeling the dynamics of small-scale river and creek plumes in tidal waters. J. Geophys. Res. – Oceans 123, http://dx.doi.org/10.1029/2019JC015737.

Spicer, P., Cole, K., Huguenard, K., MacDonald, D., Whitney, M., 2021. The effect of bottom-generated tidal mixing on tidally pulsed river plumes. J. Phys. Oceanogr. 51, 2223–2241.

Guihou, K., Polton, J., Harle, J., Wakelin, S., O'Dea, E., Holt, J., 2017. Kilometric scale modeling of the north west European Shelf Seas: Exploring the spatial and temporal variability of internal tides. J. Geophys. Res. Oceans 123, http://dx.doi.org/10.1002/2017JC012960.

Madec, G., 2008. NEMO Ocean Engine. Note Pole Model 27, ISSN: 1288-2049.

Hersbach, H., Bell, B., Berrisford, P., Hirahara, S., Horányi, A., Muñoz-Sabater, J., Nicolas, J., Peubey, C., Radu, R., Schepers, D., Simmons, A., Soci, C., Abdalla, S., Abellan, X., Balsamo, G., Bechtold, P., Biavati, G., Bidlot, J., Bonavita, M., deChiara, G., Dahlgren, P., Dee, D., Diamantakis, M., Dragani, R., Flemming, J., Forbes, R., Fuentes, M., Geer, A., Haimberger, L., Healy, S., Hogan, R., Hólm, E., Janisková, M., Keeley, S., Laloyaux, P., Lopez, P., Lupu, C., Radnoti, G., deRosnay, P., Rozum, I., Vamborg, F., Villaume, S., Thépaut, J.-N., 2020. The ERA5 global reanalysis. Q. J. R. Meteorol. Soc. 146, 1999–2049.

Chelton, D., DeSzoeke, R., Schlax, M., Nagger, K., Siwertz, N., 1998. Geographical variability of the First Baroclinic Rossby Radius of Deformation. J. Phys. Oceanogr. 28, 433–460.

Holt, J., Hyder, P., Ashworth, M., Harle, J., Hewitt, H., Liu, H., New, A., Pickles, S., Porter, A., Popova, E., Allen, J., Siddorn, J., Wood, R., 2017. Prospects for improving the representation of coastal and shelf seas in global ocean models. Geosci. Model Dev. 10, 499–523.

King, R., While, J., Martin, M., Lea, D., Lemieux-Dudon, B., Waters, J., O'Dea, E., 2018. Improving the initialization of the Met Office operational shelf-seas model. Ocean Model. 130, 1–14.

Lenhart, H.-J., Mills, D., Baretta-Bekker, H., van Leeuwen, S., van der Molen, J., Baretta, J., Blaas, M., Desmit, X., Kühn, W., Lacroix, G., Los, H., Ménesguen, A., Neves, R., Proctor, R., Ruardij, P., Skogen, M., Vanhoutte-Brunier, A., Villars, M., Wakelin, S., 2010. Predicting the consequences of nutrient reduction on the eutrophication status of the North Sea. J. Mar. Syst. 81 (1–2), 148–170.

Vörösmarty, C., Fekete, B., Meybeck, M., Lammers, R., 2000. Global systems of rivers: Its role in organizing continental land mass and defining land-to-ocean linkages. Glob. Biogeochem. Cycles 14 (2), 599–621.

Young, E., Holt, J., 2007. Prediction and analysis of long-term variability of temperature and salinity in the Irish Sea. J. Geophys. Res.- Oceans 112, http://dx.doi.org/10.1029/2005JC003386.

Warrick, J., Fong, D., 2004. Dispersal scaling from the worlds rivers. Geophys. Res. Lett. 31, http://dx.doi.org/10.1029/2003GL019114.

Lane, R., Coxon, G., Freer, J., Seibert, J., Wagener, T., 2022. A large-sample investigation into uncertain climate change impacts on high flows across Great Britain. Hydrol. Earth Syst. Sci. 26, 5535–5554.

Bowers, M., Tung, W., Gao, J., 2012. On the distributions of seasonal river flows: Lognormal or power law? Waters Resour. Res. 48, http://dx.doi.org/10.1029/2011WR011308.

Lindström, G., Pers, C., Rosberg, J., Strömqvist, J., Arheimer, B., 2010. Development and testing of the HYPE (Hydrological Predictions for the Environment) water quality model for different spatial scales. Hydrol. Res. 41, 295–319.

Davies, A., Heaps, N., 1980. Influence of the Norwegian Trench on the wind-driven circulation of the North Sea. Tellus 32, 164–175.

Pingree, R., Griffiths, D., 1980. Currents driven by a steady uniform wind stress on the shelf seas around the British Isles. Ocean. Acta 3 (2), 227–236.

Ikeda, M., Johannessen, J., Lygre, K., Sandven, S., 1989. A process study of mesoscale meanders and eddies in the Norwegian Coastal Current. J. Phys. Oceanogr. 19, 20–35.

Yankovsky, A., Chapman, D., 1997. A simple theory for the fate of buoyant coastal discharges. J. Phys. Oceanogr. 27, 1386–1401.

Lea, D., While, J., Martin, M., Weaver, A., Storto, A., Chrust, M., 2022. A new global ocean ensemble system at the Met Office: Assessing the impact of hybrid data assimilation and inflation settings. Q. J. R. Meteorol. Soc. 148, 1996–2030.

Waters, J., Lea, D., Martin, M., Mirouze, I., Weaver, A., While, J., 2015. Implementing a variational data assimilation system in an operational 1/4 degree global ocean model. Q. J. R. Meteorol. Soc. 141, 333–349.

King, R., Lea, D., Martin, M., Mirouze, I., Heming, J., 2019. The imapct of Argo observations in a global weakly coupled ocean-atmosphere data assimilation and short-range prediction system. Q. J. R. Meteorol. Soc. 146, 401–414.